Physical Medicine & Rehabilitation Journal
ISSN# 2834-3247

Research Article

Development of the Gait Events Detection Algorithm without Accurate Global Coordinate System

Kim J[1*], You H[1], Moon Y[2], Bae H[3], Ahn H[4], Jeon J[5], Seok J[1] and Bae E[1,2]

[1]REMO Inc., Republic of Korea

[2]Departments of Biomedical Engineering, University of Ulsan College of Medicine, Republic of Korea

[3]Department of Rehabilitation Medicine, Ewha Womans University Mokdong Hospital, Republic of Korea

[4]Department of Sport & Leisure Studies, Division of Arts & Health, Myongji College, Republic of Korea

[5]ESPOTEC Co., Ltd., Republic of Korea

ARTICLE INFO

Received Date: June 10, 2024
Accepted Date: June 25, 2024
Published Date: June 26, 2024

KEYWORDS

Gait analysis; 3d pose estimation; Gait events

Citation for this article: Kim J, You H, Moon Y, Bae H, Ahn H, Jeon J, Seok J and Bae E. Development of the Gait Events Detection Algorithm without Accurate Global Coordinate System. Physical Medicine & Rehabilitation Journal. 2024; 6(1):134

Corresponding author:
Kim J,
REMO Inc., Republic of Korea, Tel: +82-70-7575-3856;
Email: astasdf@gmail.com

ABSTRACT

Gait analysis plays a crucial role in assessing human movement patterns and identifying potential abnormalities. Traditional methods for gait analysis involve complex setups, such as attaching markers and using multiple cameras, making them cumbersome and time-consuming. Recent advancements in artificial intelligence (AI) have opened up possibilities for analyzing gait using single-camera videos. However, existing approaches rely on ground information and lack the ability to detect gait events accurately. In this study, we present a novel algorithm for automatically detecting gait events without the need for accurate global coordinate systems. Our algorithm utilizes joint angles and relative distances between key points to detect gait cycles and events. To validate our algorithm, we participated 34 healthy male subjects. Three-dimensional motion capture systems were used to measure joint movements during walking, while a 2D camera recorded the entire measurement space. The gait events detected by our algorithm were compared with visually defined events by an expert examiner. The results demonstrated that our algorithm successfully detected all gait events. The comparison analysis showed an absolute constant error of 1.04 frames (17.4ms) for hell strike detection and 1.29 frames (21.5ms) for toe off detection. Furthermore, the gait cycle variables calculated from 2D camera images using our algorithm showed no statistical difference compared to those measured visually using a 3D motion capture system.

Overall, our study presents a promising algorithm for gait event detection without relying on ground information. By leveraging joint angles and relative distances, our algorithm can accurately detect gait cycles and events, enabling gait analysis from wild images. This research contributes to the development of AI-based gait analysis techniques, offering potential applications in clinical assessments and fall risk evaluations. Further improvements can be made to enhance the algorithm's performance in handling acceleration and deceleration sections during gait analysis.

INTRODUCTION

Gait is a natural movement of the human body to move from one place to another, and it utilizes various functions, any of which can affect gait [1]. Gait speed is affected by both functional and physiological changes [2-3] and is often used to measure fall risk [3,4]. The gold standard for gait analysis is 3D motion analysis, which involves placing infrared reflective markers on anatomical locations throughout the body and using multiple infrared cameras to measure human coordinates in three-dimensional space. This method is accurate, but it is cumbersome to attach markers and has the disadvantage of calibrating the three-dimensional space with multiple cameras [5]. To analyze gait using the three-dimensional coordinates of the human body, gait events must first be detected. The current gold standard for the automatic detection of gait events is the use of ground reaction forces measured by force platforms [6,7]. However, this method not only requires the installation of force platforms, but also has the disadvantage of being inaccurate for pathological gaits such as foot drags [7]. Many gait event detection algorithms using kinematic data have been developed to analyze gait in various situations [8-14]. However, these algorithms basically require ground information including 3D coordinates.

Recently, there have been studies that attempted to analyze gait in wild videos using advanced Artificial Intelligence (AI) [15-19]. Most of them extract gait features based on silhouette to determine the gait state or perform gait recognition [16-18]. Bouchrika and Nixon [15] detected gait events and analyzed the joint angles of the gait cycle, but the camera angle had to be fixed and only 2D motions were analyzed. Recently, many artificial intelligence methods have been studied to accurately estimate 3D pose from 2D wild images [20-23]. Various approaches such as graph convolutional neural network [21], transformer [22], and 2.5D heatmap [23] have been studied for high accuracy. As a result of these studies, the accuracy of Mean Per Joint Position Error (MPJPE) is very high with less than 100mm. Therefore, it is thought that gait analysis using single camera video is possible. However, 3D pose estimated from wild images has no ground information. Thus, it is difficult to apply the gait events detection algorithms. Therefore, in this study, we developed an algorithm that automatically detects the gait events without the ground information for the 3D pose data from wild images.

METHODS

Gait event detection algorithm

To detect the gait events without an accurate global coordinate system, we developed an algorithm using only joint angles and relative distances between keypoints. We also designed the algorithm to detect gait cycles first and then detect gait events (Figure 1).

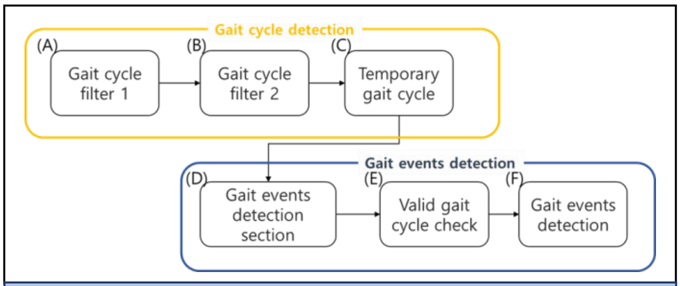

Figure 1: Block diagram of gait event detection algorithm.
(A) Gait cycle filter 1 is the cross-correlation of hip joint sagittal plane angle and cosine wave. (B) Gait cycle filter 2 is the cross-correlation of distance between the ankles (inter-ankle distance) and cosine wave. (C) Temporary gait cycle is an algorithm that determines a temporary gait cycle based on the inter-ankle distance when gait cycle filter 1 and 2 are matched. (D) Gait events detection section sets the area to detect gait events based on the peak points of the inter-ankle distance. (E) Valid gait cycle check is an algorithm that recognizes a normal gait cycle when the pelvic-ankle distance in the vertical direction in pelvis orientation decreases by more than a certain value in each gait events detection section. (F) gait events detection is an algorithm that detects heel strike by searching the inter-ankle distance in time order in the gait events detection section and detects toe off by searching in reverse time order.

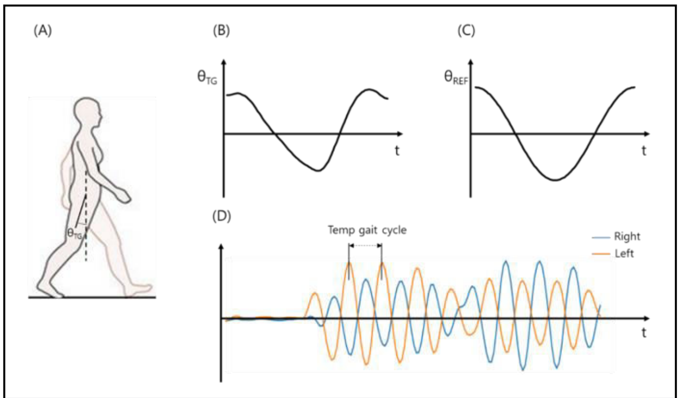

Figure 2: First cross-correlate filter.
(A) Target angle(θ_{TG}) is the sagittal hip joint angle. (B) θ_{TG} according to the gait cycle. (C) Reference angle (θ_{REF}) according to the gait cycle. Data Variation by the cadence. (D) Cross-correlate coefficient of θ_{TG} and θ_{REF} over time. Positive peak to positive peak can be set as temp gait cycle.

Gait cycle detection: To detect gait cycles, we used hip joint sagittal plane angle, inter-ankle distance, and pelvic-ankle distance. First, the hip joint sagittal plane angle was cross-correlated with the cosine wave by cadence and the temporary cycle was selected when it showed high agreement (Figure 2). Second, the temporary cycle was selected when the distance between the ankles (inter-ankle distance) showed high agreement by calculating the cross-correlate with the cosine wave by cadence (Figure 3). When two temporary cycles matched, we set the temporary gait cycle to be between two positive peaks in the inter-ankle distance when the inter-ankle distance at that point showed one negative peak between the two positive peaks.

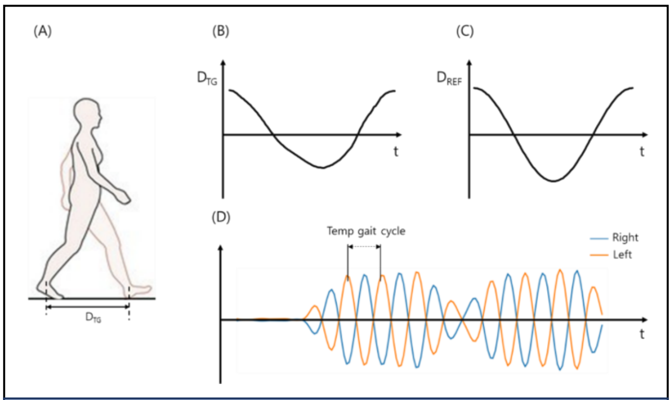

Figure 3: Second cross-correlate filter.
(A) Target distance (D_{TG}) is inter-ankle distance in the anterior-posterior direction in pelvis orientation. (B) D_{TG} according to the gait cycle. (C) Reference distance (D_{REF}) according to the gait cycle. Data Variation by the cadence. (D) Cross-correlate coefficient of D_{TG} and D_{REF} over time. Positive peak to positive peak can be set as temp gait cycle.

Gait event detection: The gait events detection section was set from the peaks of the temporary gait cycle to the previous opposite direction peak. The first positive peak was categorized as the previous gait events detection section, the negative peak as the opposite gait events detection section, and the last positive peak as the current gait events detection section (Figure 4).

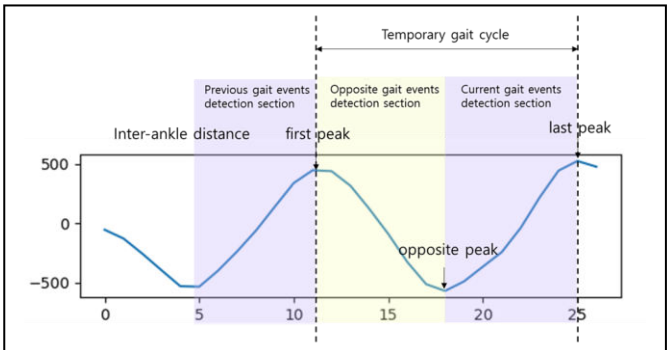

Figure 4: Gait events detection section.

In each gait events detection section, the normal gait cycle was judged when the pelvic-ankle distance in the vertical direction in pelvis orientation decreased by more than a certain distance (ex: 30mm) (Figure 5).

Then, the algorithm to find the correct gait events (heel strike (HS) and toe off (TO)) was applied for around each HS of gait cycle. If the algorithm could not find the HS or TO, all gait events of that gait cycle was disregarded. In the algorithm, TO be set as the latest of the time when the amplitude of the inter-ankle distance was 15% and the time when the slope of the inter-ankle distance reached 20% based on the maximum value. HS was set as the earliest of the time when the amplitude of the inter-ankle distance was 95% and slope less than 20% time of maximum slope for inter-ankle distance (Figure 6).

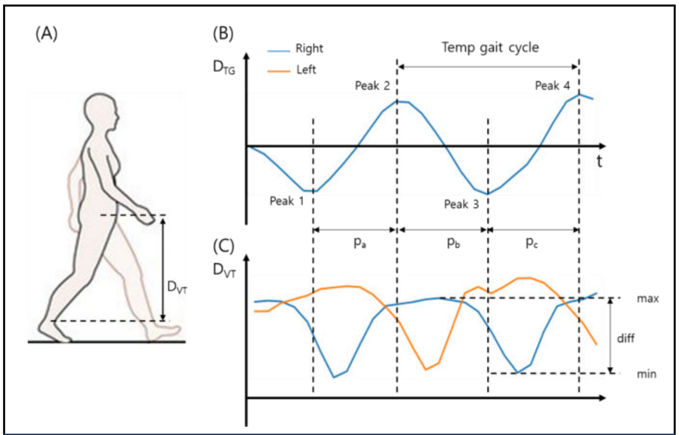

Figure 5: Gait cycle validation algorithm.
(A) Vertical distance (D_{VT}) is pelvic-ankle distance in the vertical direction in pelvis orientation. (B) D_{TG} according to the gait cycle. The temporary gait cycle of the foot can be identified between positive peaks and positive peaks, and the temporary gait cycle of the opposite foot can be identified between negative peaks and negative peaks. (C). The amount of change was checked by the difference between the min and max of D_{VT} within the temporary gait cycle, and it was decided that the difference should be more than a certain distance to be considered as a valid gait cycle.

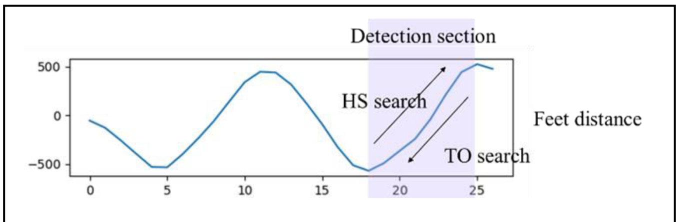

Figure 6: Gait event detection algorithm.

Subjects

Thirty-four healthy males with no history of lower limb disorders participated in this study (age: 20.8 ± 4.8 years, height: 176.4 ± 5.5 cm, weight: 74.8 ± 10.7 kg). All subjects provided written informed consent on a form that had been approved by the Public Institutional Review Board Designated by Ministry of Health and Welfare (P01-202205-01-002; date of registration: May 2, 2022). All data collection began on June 1, 2022 and ended on June 30, 2022.

Experimental Procedure

A 3D motion capture system (8 cameras, Prime 41, OptiTrack, NaturalPoint, USA) was used to measure human joint movements during walking. The markerset was Motive Software's Baseline + Hinged Toe markerset [24] and was acquired at 60 Hz. The system was calibrated before measuring gait. The 2D camera (OBSBOT Tiny, OBSBOT, HongKong) was positioned to capture the entire measurement space and recorded at 30 Hz. The camera was taken parallel to the ground in the side of the measurement space. Subjects performed 10 gait trials on a 4m walkway and 3 treadmill gait trials at a 4km/h speed with one minute duration. The 10 level gait trials consisted of 2 left, 1 front-left, 1 front, 1 front-right, 2 right, 1 back-right, 1 back, 1 back, and 1 back-left, based on camera view.

Data analysis

For verification, the gait events for 3D joint positions from motion capture system were defined visually by an experience examiner and compared it with gait events detected by the developed algorithm. An experience examiner defined HS using the vertical coordinates of the heel marker and TO using the vertical coordinates of the toe marker while observing the entire three-dimensional posture during walking. To verify the accuracy of the developed algorithm in detecting gait events, the joint coordinates measured from the 3D motion capture system were compared with a gold standard visually detected by an expert and the gait events detected by the developed algorithm. 3D human keypoints were estimated in SMPL24 [25] format using MeTRAbs [23] from 2D camera images, and the developed gait event detection algorithm was applied. The 2D camera footage was only measured during flat walking. There were many cases where the AI could not recognise the human body normally because the subject was wearing a full-body black suit. Due to this, only 337 gait cycles out of a total of 1235 gait cycles were used for the comparison analysis. Since the 2D camera was not synchronised with the 3D motion capture system, cycle duration, stance phase and double support phase were compared using t-tests. The significance level for all statistics was set at 0.05.

RESULTS

As a result, all gait events were detected by the developed algorithm. Comparison between visual and the developed algorithm showed that the absolute constant error was 1.04 frames, i.e., 17.4ms of error, for heel-strike detection and 1.29 frames, i.e., 21.5ms of error, for toe-off detection. The results showed that all gait events detected by visually through joint coordinates measured by the 3D motion capture system were also detected by the developed algorithm. The absolute constant error of the visual and developed algorithms was 1.30 frames for HS and 1.46 frames for TO in level gait, and 0.73 frames for HS and 0.98 frames for TO in treadmill gait (Table 1). In level gait, HS and TO were detected a total of 1235 times each, with 95.5% of HS and 97.6% of TO events having a frame difference of 3 or less between visual and the developed algorithm (Figure 7). In treadmill gait, HS and TO were detected a total of 3023 times, with 99.2% HS and 99.2% TO for events with a frame difference of 3 or less between visual and the developed algorithm (Figure 8).

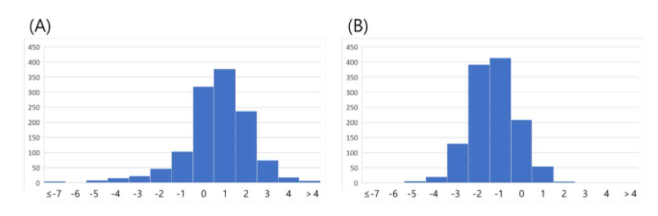

Figure 7: Histogram of frame difference for visual and algorithm detected gait events from level gait. (A)HS (B) TO.

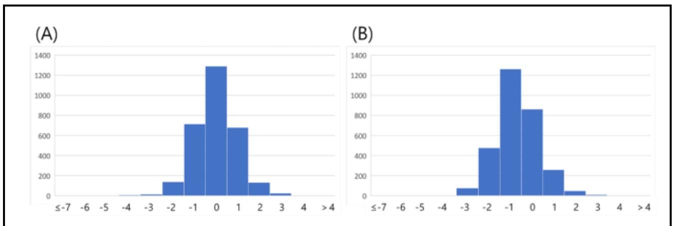

Figure 8: Histogram of frame difference for visual and algorithm detected gait events from treadmill gait. (A)HS (B) TO.

Cycle duration, stance phase and double support phase calculated from human keypoints in 2D camera images were 1.16s, 69.7% and 20.0%, respectively, which were not statistically different from 1.16s, 69.8% and 19.9% measured visually in 3D motion capture system.

Table 1: Comparison of gait cycles visually measured by a 3D motion capture system with the developed algorithm.

		Frame	MS
Total	HS	1.04	17.4
	TO	1.29	21.5
Level gait	HS	1.30	21.7
	TO	1.46	24.3
Treadmill gait	HS	0.73	12.1
	TO	0.98	16.4

DISCUSSION

In this study, we aimed to develop an algorithm that can analyze the gait cycle in the absence of a three-dimensional coordinate system for the ground. The results showed that the average error was accurate to within 2 frames for level gait and 1 frame for treadmill gait. In this study, the gait cycle algorithm showed a large error due to a lot of acceleration/deceleration sections, including start and stop within a 4-meter walkway. In future study, it is necessary to improve the algorithm to recognize acceleration/deceleration sections and analyze the gait cycle more accurately.

All parameters used in the developed algorithm are joint angles, anterior-posterior and vertical distances based on the pelvic coordinate system but those related with the three-dimensional coordinate system with respect to the ground are not used. First, the hip joint angle was used to check for periodicity. DeAsha et al. [14] detected HS as the peak of the contralateral foot hip joint angle, but it showed poor performance because it failed to consider pathological gait [26]. In this study, hip joint angle was only used to check periodicity by considering pathological gait. Inter-ankle distance in the anterior-posterior directions was used for periodicity check and detailed detection of HS and TO. Since the algorithm was designed to analyze data without information about the ground and the direction of walking, the direction of walking was assumed based on the coordinate system of the pelvis. This resulted in the acquisition of noisy signals at the exact heading distance, so it was difficult to directly apply the foot coordinate peak detection [8,13], velocity peak detection [10,12], and velocity threshold [9] of existing algorithms. We needed an algorithm that is robust to noise, so we configured two conditions: amplitude of foot distance and slope change. The vertical movement of the foot was assumed to be the pelvic-ankle distance in the vertical pelvic coordinate system and used to determine the validity of the gait cycle.

In both level gait and treadmill gait, TOs were characterized by an overall delay of 1-2 frames in detection (Figure 6, 7). This was likely caused by setting the amplitude condition for TO detection to 15%. We set a high threshold of 15% to account for pelvic rotation, propulsion, and changes in pathological gait, but it did not work well in a normal gait environment. It is necessary to find the optimal threshold by applying it to pathological gait in the future.

We applied the gait cycle detection algorithm by extracting AI 3D human key points from 2D videos taken with a 3D motion capture system, and confirmed that there was no significant statistical difference when comparing the results with the motion capture results (Table 2). Even though only 337 out of 1235 gait cycles (27%) were successfully analyzed, and the analyzed data contained a lot of noise due to large deviations, we were able to confirm the possibility of gait analysis in wild images, and it is expected that more accurate analysis will be possible if AI human pose estimation is further developed in the future.

Table 2: Comparing gait cycle variables in 2D camera with AI and 3D motion capture.

	Condition		P
	3D Motion Capture	2D Camera + AI	
Cycle duration (s)	1.16 (0.006)	11.6 (0.007)	0.16
Stance phase (%)	69.9 (2.65)	69.8(16.47)	0.34
Double support phase (%)	19.9 (3.80)	20.2 (17.05)	0.12

STATEMENTS AND DECLARATIONS

Funding

This study was carried out with the support of ´R&D Program for Forest Science Technology (Project No. 2021404B10-2223-0107) ´ provided by Korea Forest Service (Korea Forestry Promotion Institute).

Competing Interests

The authors have no relevant financial or non-financial interests to disclose.

Author Contributions

All authors contributed to the study conception and design. Material preparation, data collection and analysis were performed by Jungyoon Kim, Hyeonseok You, Youngjin Moon, Hasuk Bae, Hyunkyun Ahn, Jeonghoon Jeon, Jaewoo Seok and EunKyung Bae. The first draft of the manuscript was written by Jungyoon Kim and all authors commented on previous versions of the manuscript. All authors read and approved the final manuscript.

Ethics approval

This study was performed in line with the principles of the Declaration of Helsinki. Approval was granted by the Public Institutional Review Board Designated by Ministry of Health and Welfare (P01-202205-01-002; date of registration: May 2, 2022).

Consent to participate

Written informed consent was obtained from the parents.

REFERENCES

1. Perry J, Burnfield J. (2010). Gait Analysis: Normal and Pathological Function. J Sports Sci Med. 9-353.
2. Albert JA, Owolabi V, Gebel A, Brahms CM, Granacher U, et al. (2020). Evaluation of the Pose Tracking Performance of the Azure Kinect and Kinect v2 for Gait Analysis in Comparison with a Gold Standard: A Pilot Study. Sensors (Basel). 20: 5104.
3. Fritz S, Lusardi M. (2009). White paper: “walking speed: the sixth vital sign”. J Geriatr Phys Ther. 32: 2-5.
4. Guimaraes RM, Isaacs B. (1980). Characteristics of the gait in old people who fall. Int Rehabil Med. 2: 177-180.
5. Simon SR. (2004). Quantification of human motion: gait analysis—benefits and limitations to its application to clinical problems. J Biomech. 37: 1869-1880.
6. Veilleux LN, Raison M, Rauch F, Robert M, Ballaz L. (2016). Agreement of spatio-temporal gait parameters between a vertical ground reaction force decomposition algorithm and a motion capture system. Gait & posture. 43: 257-264.
7. Lempereur M, Rousseau F, Rémy-Néris O, Pons C, Houx L, et al. (2020). A new deep learning-based method for the detection of gait events in children with gait disorders: Proof-of-concept and concurrent validity. J Biomech. 98: 109490.
8. Zeni JA, Richards JG, Higginson JS. (2008). Two simple methods for determining gait events during treadmill and overground walking using kinematic data. Gait Posture. 27: 710-714.
9. Ghoussayni S, Stevens C, Durham S, Ewins D. (2004). Assessment and validation of a simple automated method for the detection of gait events and intervals. Gait Posture. 20: 266-272.
10. Hreljac A, Marshall RN. (2000). Algorithms to determine event timing during normal walking using kinematic data. J. Biomech. 33: 783-786.
11. Jasiewicz JM, Allum JHJ, Middleton JW, Barriskill A, Condie P, et al. (2006). Gait event detection using linear accelerometers or angular velocity transducers in able-bodied and spinal-cord injured individuals. Gait Posture 24: 502-509.
12. O’Connor CM, Thorpe SK, O’Malley MJ, Vaughan CL. (2009). Automatic detection of gait events using kinematic data. Gait Posture. 25: 469-474.
13. Desailly E, Daniel Y, Sardain P, Lacouture P. (2009). Foot contact event detection using kinematic data in cerebral palsy children and normal adults gait. Gait Posture. 29: 76-80.
14. De Asha AR, Robinson MA, Barton GJ. (2012). A marker based kinematic method of identifying initial contact during gait suitable for use in real-time visual feedback applications. Gait Posture. 36: 650-652.
15. Bouchrika I, Nixon MS, editors. (2007). Model-based feature extraction for gait analysis and recognition. MIRAGE. 4418: 150-160.
16. Gupta A, Jadhav A, Jadhav S, Thengade A. (2020). Human gait analysis based on decision tree, random forest and KNN algorithms. Applied Computer Vision and Image Processing: Proceedings of ICCET 2020, Volume 1. Singapore: Springer Singapore. 283-289.
17. Khan MA, Kadry S, Parwekar P, Damaševičius R, Mehmood A, et al. (2021). Human gait analysis for osteoarthritis prediction: a framework of deep learning and kernel extreme learning machine. Complex Intell Syst. 9: 2665-2683.
18. Wang Y, Xia Y, Zhang Y. (2022). Beyond view transformation: feature distribution consistent GANs for cross-view gait recognition. The Visual Computer. 38: 1915-1928.
19. Sugiyama Y, Uno K, Matsui Y. (2023). Types of anomalies in two-dimensional video-based gait analysis in

uncontrolled environments. PLOS Computational Biology. 19: e1009989.

20. Bogo F, Kanazawa A, Lassner C, Gehler P, Romero J, et al. (2016). Keep it SMPL: Automatic estimation of 3D human pose and shape from a single image. In Computer Vision–ECCV 2016: 14th European Conference, Amsterdam, The Netherlands, October 11-14, 2016, Proceedings, Part V 14. Springer International Publishing. 561-578.
21. Choi H, Moon G, Lee KM. (2020). Pose2mesh: Graph convolutional network for 3d human pose and mesh recovery from a 2d human pose. In Computer Vision–ECCV 2020: 16th European Conference, Glasgow, UK, August 23–28, 2020, Proceedings, Part VII 16. Springer International Publishing. 769-787
22. Lin K, Wang L, Liu Z. (2021). End-to-end human pose and mesh reconstruction with transformers. In Proceedings of the IEEE/CVF conference on computer vision and pattern recognition. 1954-1963.
23. Sárándi I, Linder T, Arras KO, Leibe B. (2020). Metrabs: metric-scale truncation-robust heatmaps for absolute 3d human pose estimation. IEEE Transactions on Biometrics, Behavior, and Identity Science. 3: 16-30.
24. (2023)Baseline + Hinged Toe (41) [Internet]. Corvallis: NaturalPoint.
25. Loper M, Mahmood N, Romero J, Pons-Moll G, Black MJ. (2015). SMPL: A skinned multi-person linear model. ACM transactions on graphics (TOG). 34: 1-16.
26. Bruening DA, Ridge ST. (2014). Automated event detection algorithms in pathological gait. Gait & posture. 39: 472-477.